

A broadband signal recycling scheme for saturating quantum limit from optical losses

Teng Zhang, Joe Bentley, and Haixing Miao

¹*School of Physics and Astronomy, and Institute of Gravitational Wave Astronomy,
University of Birmingham, Edgbaston, Birmingham B15 2TT, United Kingdom*

Quantum noise limits the sensitivity of laser interferometric gravitational-wave detectors. Given the state-of-the-art optics, the optical losses define the lower bound of the best possible quantum-limited detector sensitivity. In this work, we come up with a broadband signal recycling scheme which gives potential solution to saturate this lower bound by converting the signal recycling cavity to be a broadband signal amplifier using an active optomechanical filter. We will show the difference and advantage of such a scheme compared with the previous white-light-cavity scheme using the optomechanical filter in [Phys.Rev.Lett.115.211104 (2015)]. The drawback is that the new scheme is more susceptible to the thermal noise of the mechanical oscillator, which is challenging on the mechanical property of the oscillator.

I. INTRODUCTION

The optical losses are unavoidable in real detectors and can come from various sources, *e.g.* absorption, scattering, mode mismatch and the open ports which are necessary to extract error signals for sensing and control purpose. Depending on the mechanism how optical losses couple to the gravitational-wave signal channel, they can be classified into internal loss, including the arm cavity loss ϵ_{arm} ; signal-recycling cavity (SRC) loss ϵ_{SRC} ; and external loss in the output chain ϵ_{ext} . The spectral density of these optical losses is given by [1]:

$$S_\epsilon = \frac{\hbar c^2}{4L^2\omega_0 P_{\text{arm}}} \left[\epsilon_{\text{arm}} + \frac{(\Omega^2 + \gamma_{\text{arm}}^2)T_{\text{ITM}}}{4\gamma_{\text{arm}}^2} \epsilon_{\text{SRC}} + \frac{1}{4}T_{\text{SRC}}\epsilon_{\text{ext}} \right], \quad (1)$$

where ω_0 is the laser frequency, Ω is the angular frequency of gravitational wave signals, L is the arm length, P_{arm} is the arm cavity power, T_{ITM} is the input test mass (ITM) transmissivity, $\gamma_{\text{arm}} = cT_{\text{ITM}}/(4L)$ is the arm cavity bandwidth and T_{SRC} is the effective transmissivity of the signal-recycling cavity (SRC) formed by ITM and the signal-recycling mirror (SRM). The arm cavity loss limited sensitivity is frequency independent, since the vacuum mixes with the signals directly inside the arm cavity. In contrast, the SRC loss limited sensitivity rises at higher frequencies above the arm cavity bandwidth due to the decrease of signal response. It is independent of any optical modules inside the SRC. The external loss happens on the output path of the interferometer, where there are unwanted effects including the mode mismatch at the output mode cleaner, and an imperfect quantum efficiency of the photodiode. The output loss noise depends on the SRC parameters and T_{SRC} equals to 0.14 in advanced LIGO (aLIGO). Apparently, it also limits the observed squeezing level. For example, with 10% external loss, the observed squeezing cannot be more than 10 dB. Fig. 1 shows the optical-loss limits for aLIGO [2].

From Eq. (1), we learn that at high frequencies, *i.e.* $\Omega \gg \gamma_{\text{arm}}$, the best achievable quantum sensitivity is

limited by the SRC loss with spectral density

$$S_{hf} = \frac{\hbar\Omega^2}{\omega_0 P_{\text{arm}} T_{\text{ITM}}} \epsilon_{\text{SRC}}, \quad (2)$$

which turns out to be independent of the arm length. It is then exciting and crucial to explore the way of saturating the high frequency quantum limit, which will give the maximal astrophysical outcome, in particular on neutron star physics [3, 4]. As shown in Fig. 1, the sensitivity of aLIGO with 9 dB observed squeezing is still one order of magnitude worse than the SRC loss limit with $\epsilon_{\text{SRC}} = 1000 \text{ ppm}$ in the frequency range of 1-5 kHz.

Up to now, the proposed quantum techniques can be categorized into the following two classes: (1) noise suppression/cancellation schemes; (2) signal amplification schemes. The strategies that allow us to overcome

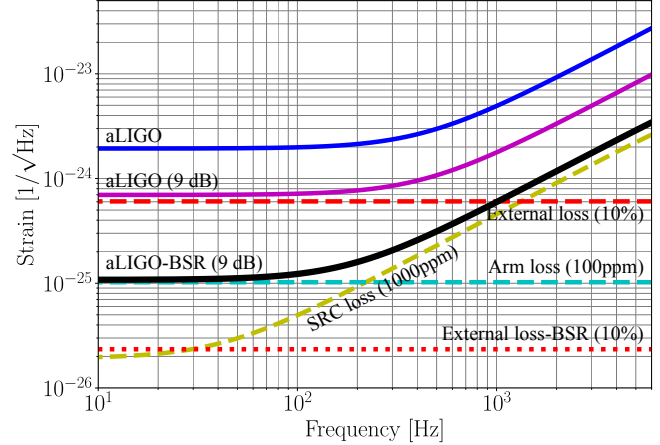


FIG. 1. This figure shows the noise spectral densities of optical losses and the shot noise limited sensitivity with parameters from aLIGO configuration. We assumed 1000 ppm SRC loss, 100 ppm arm cavity loss and 10% external loss. The blue line illustrates the shot noise of aLIGO. The purple line is with ~ 9 dB observed squeezing (15dB squeezing in the arm cavities). The black line illustrates the resulting shot noise of the aLIGO configuration with the BSR scheme discussed in this work. It saturates the SRC loss limit at high frequencies and arm cavity loss limit at low frequencies.

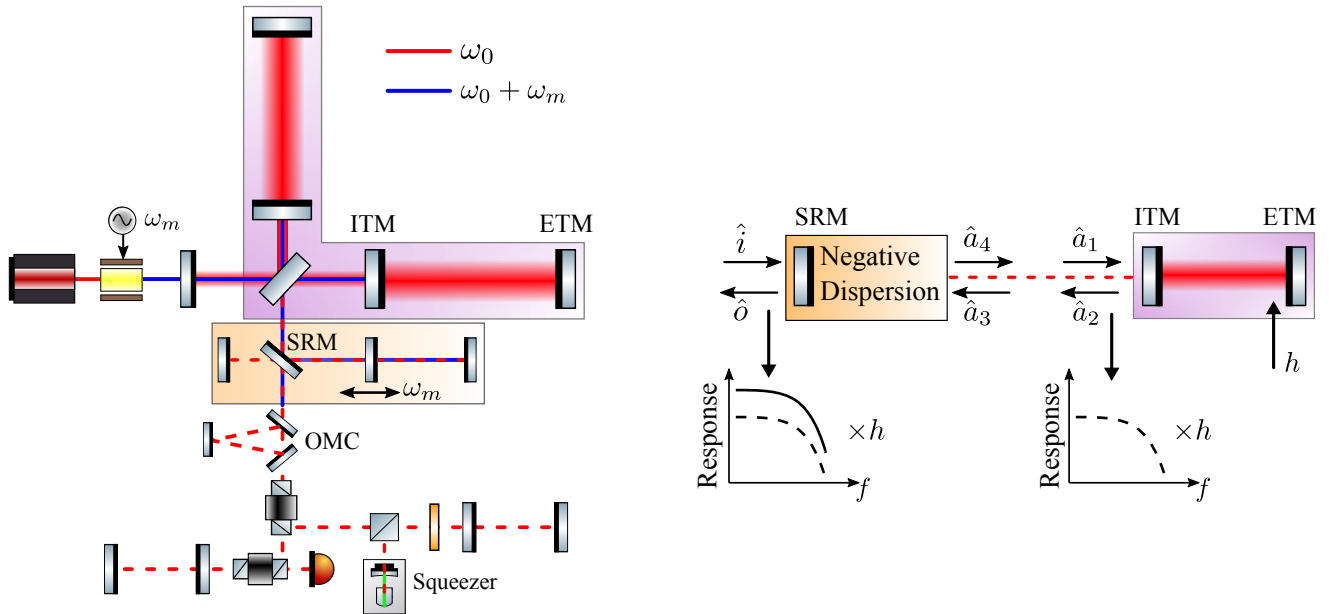


FIG. 2. Left: Gravitational wave detector with the proposed broadband signal recycling scheme and input/output filter cavities. The carrier laser is at ω_0 (red). The optomechanical filter cavity is pumped with a laser at $\omega_0 + \omega_m$ (blue), which comes from modulating the input carrier and transmits to the dark port under the Schnupp asymmetry. The mechanical frequency of the oscillator of the optomechanical filter cavity is ω_m . The blue beam is filtered with an output mode cleaner (OMC). The input and output filter cavity are placed for frequency dependent squeezing and variational readout. Right: Simplified schematic of the broadband signal recycling scheme. Inside the SRC, the phase of sidebands reflecting from the arm cavity is cancelled, thus the SRC is on resonance in a broad frequency band. The SRC is converted to be an amplifier for the signals coming out from the arm cavity with a gain of $1/\sqrt{T_{\text{SRM}}}$.

the standard quantum limit are known as *Quantum-nondemolition techniques* [5, 6], for example, frequency dependent squeezing and variational readout [7]. Based on the understanding from the optical-loss limit, despite utilizing internal or external squeezing [8–11] for the purpose of noise suppression, the observed squeezing level has an unsurpassed bound due to external loss. The signal enhancement scheme can potentially complement the squeezing for achieving the loss limit. The most well-known signal amplification technique, which has already been implemented in the second-generation detectors, is the SRC. Obviously, both the high-frequency and low-frequency sensitivity improve on *Resonant Sideband Extraction* mode. However, this comes with a price of sacrificing the peak sensitivity at intermediate frequency. It is due to the accumulation of the phase of the sidebands traveling inside the cavity (positive dispersion), which leads to the destructive interference of sidebands whose frequencies are larger than the cavity bandwidth. Another recent work on high-frequency detector design uses the coupled-cavity resonance of the arm cavity and the SRC. That scheme gives rise to a narrow band dip in the noise spectrum at high frequencies [4, 12]. Such a coupled-cavity resonance shows up when the sidebands resonate within the SRC. The sidebands in the SRC can only resonate in a narrow high frequency band. Equivalently, the identical resonance condition is satisfied at carrier frequency when the SRC is tuned on the *Signal*

Recycling mode.

One strategy to broaden up the bandwidth without sacrificing the peak sensitivity is to introduce negative dispersion to cancel the arm cavity round trip phase $2\Omega L/c$, by means of white light cavities [13–15]. However, the negative phase provided by the unstable filter cavity in [14] evolves exponentially as a function of frequency. As it turns out, there is an imperfect phase cancellation outside the frequency band of validity of the linear approximation to the exponential function, which eventually leads to a rapid decrease of sensitivity above a certain frequency.

The coupled SRC and arm cavity design and white light cavity idea are heuristic. The scheme proposed in this work realises the coupled SRC and arm cavity resonance in a broad frequency band. We name it as the broadband signal recycling (BSR) scheme.

II. DESIGN CONCEPT AND QUANTUM NOISE

The scheme we propose in this work is shown in Fig. 2. Inside the SRC, an optomechanical filter cavity which provides the negative dispersion is placed for canceling the phase gained by the sidebands upon reflection from the arm cavity. The optomechanical filter cavity is pumped with a laser at frequency $\omega_0 + \omega_m$, which is generated from modulating the input carrier. A Schnupp

asymmetry allows the carrier to transmit to the dark port. It is worthwhile to note the difference compared with the previous scheme in [14]. In that configuration, an addition mirror so-called iSRM is introduced for achieving an impedance match with the ITM, which effectively removes the ITM for the sidebands. However, as we mentioned above, the negative phase provided by the optomechanical filter cavity and the round trip phase in the arms cancel imperfectly at higher frequencies. Here we show the iSRM (extra complexity) is not required and realise an exact phase cancellation in ideal case .

In Fig. 2, the optical input/output relation of arm cavity can be derived as [7]:

$$\hat{a}_2 \approx \frac{\gamma_{\text{arm}} + i\Omega}{\gamma_{\text{arm}} - i\Omega} \hat{a}_1 = e^{i\beta} \hat{a}_1, \quad (3)$$

where $\beta = 2\text{atan} \frac{\Omega}{\gamma_{\text{arm}}}$ is the phase of the sidebands reflecting from the arm cavity. In order to cancel this frequency dependent phase inside the SRC and convert the SRC a broadband signal amplifier, we need to introduce negative phase lag. As it turns out, this can be exactly provided by an optomechanical filter in the so-called resolved-sideband regime, *i.e.* $\omega_m \gg \gamma_f \gg \Omega$, where ω_m is the mechanical resonant frequency, γ_f is the filter cavity bandwidth. When the mechanical damping rate γ_m , is much smaller than the negative mechanical damping rate due to the optomechanical interaction γ_{opt} , the optomechanical filter cavity gives the following open-loop transfer function [14]:

$$\hat{a}_{\text{out}} \approx -\frac{\gamma_{\text{opt}} - i\Omega}{\gamma_{\text{opt}} + i\Omega} \hat{a}_{\text{in}} = e^{i\alpha} \hat{a}_{\text{in}}, \quad (4)$$

where $\gamma_{\text{opt}} = P\omega_0/(m\omega_m cL_f \gamma_f)$. There is $\gamma_m = \omega_m/Q_m$. m is the mass of the mechanical oscillator, Q_m is the quality factor and P is the circulating power in the optomechanical filter. When

$$\gamma_{\text{opt}} = \gamma_{\text{arm}}, \quad (5)$$

there is an exact cancellation of α and β up to a frequency-independent constant: $\alpha + \beta = \pi$. With the signal-recycling mirror tuned to give another constant π phase shift, the short SRC is on resonance in a broad frequency band. As it turns out, $\hat{o} = \hat{a}_2/\sqrt{T_{\text{SRM}}}$, where T_{SRM} is the power transmissivity of the SRM. The effective transmissivity of the SRC is

$$T_{\text{SRC}} = \frac{T_{\text{ITM}} T_{\text{SRM}}}{(1 + \sqrt{R_{\text{ITM}} R_{\text{SRM}}})^2}, \quad (6)$$

where $R_{\text{ITM}}, R_{\text{SRM}}$ is the power reflectivity of the ITM and SRM. In the optomechanical filter cavity, the thermal noise effect of the mechanical oscillator can be modelled as an effective SRC loss [3]:

$$\epsilon_{\text{eff}} = \frac{4k_B}{\hbar\gamma_{\text{opt}}} \frac{T_{\text{env}}}{Q_m} = 1000 \text{ ppm} \times \frac{0.014}{T_{\text{itm}}} \times \frac{L}{4000 \text{ m}} \times \frac{T_{\text{env}}/Q_m}{5 \times 10^{-13}} \quad (7)$$

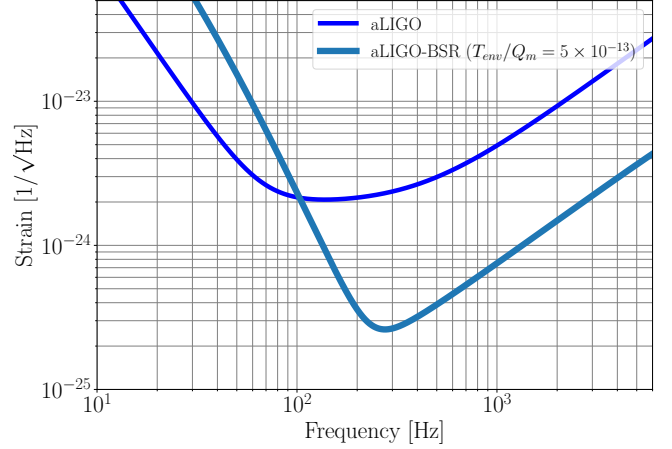


FIG. 3. This figure shows the quantum noise spectral densities of aLIGO and BSR configurations with $T_{\text{env}}/Q_m = 5 \times 10^{-13}$. 15 dB squeezing is assumed in the arm cavity and ~ 9 dB squeezing is observed under 10% external loss.

where k_B is the Boltzmann constant, T_{env} is the environmental temperature. In our case, to guarantee an additional effective SRC loss contribution smaller than 1000 ppm, T_{env}/Q_m has to be smaller than $5 \times 10^{-13} \text{ K}$. This gives an extremely stringent requirement, which is the drawback of the BSR scheme compared with the scheme in [14]. This is because the value of γ_{opt} in our scheme is smaller than that in [14], where $\gamma_{\text{opt}} = c/L$. Therefore large bandwidth of the arm cavity is preferred to implement the BSR scheme. A T_{env}/Q_m only $\sim 10^{-8}$ is demonstrated in [16]. To suppress the thermal noise in the BSR scheme is challenging.

After taking into account frequency dependent squeezing and variational readout as show in Fig. 2, the spectral density of the detector can be calculated as the sum of [17]

$$S = \frac{h_{\text{SQL}}^2}{2} \left[\frac{e^{-2r} + \epsilon_{\text{ext}}}{\mathcal{K}} + \frac{\epsilon_{\text{ext}}}{1 + \epsilon_{\text{ext}} e^{2r}} \mathcal{K} \right], \quad (8)$$

and the SRC and arm cavity loss contribution, where $e^{-2r} \approx 0.03$ represents ~ 15 dB squeezing. \mathcal{K} is the famous Kimble factor and h_{SQL} is the standard quantum limit,

$$\mathcal{K} = \frac{16\omega_0 P_{\text{arm}} \gamma_{\text{arm}} T_{\text{SRM}}}{McL\Omega^2(\gamma_{\text{arm}}^2 + \Omega^2)}, \quad h_{\text{SQL}} = \sqrt{\frac{8\hbar}{(M\Omega^2 L^2)}}. \quad (9)$$

Here M is the mass of the detector test mass. We adopt $T_{\text{SRM}} = 0.005$ and $T_{\text{ITM}} = 0.014$, thus $T_{\text{SRC}} = 0.00002$. The arm cavity power P_{arm} is 800 kW and arm length L is 4 km. The resulting shot-noise-limited sensitivity which corresponds to the sum of the first term in Eq. 8 and the loss limit is shown in Fig. 1. As we can observe, the shot noise limited sensitivity of the BSR scheme saturates the arm cavity loss limit at low frequencies and the SRC loss

limit at high frequencies. Including the radiation pressure noise, the detector sensitivities are shown in Fig. 3.

III. SUMMARY AND OUTLOOK

In this work, we show one scheme whose shot noise limited sensitivity can saturate the optical-loss limit. An optomechanical filter cavity inside the SRC provides a proper negative phase lag that cancels the frequency dependent phase of the signal sidebands when reflecting from the arm cavity. It allows the simultaneous resonance of broadband sidebands in the SRC, which can be viewed as a frequency dependent coupled-cavity resonance. Instead of suppressing the noises which will be limited by losses, the signals are amplified in this scheme. The amplification gain is $1/\sqrt{T_{SRM}}$. Note that the radiation pressure noise will also be amplified by the same amount, and the BSR scheme alone cannot overcome the

standard quantum limit. For future detectors beyond the aLIGO, using high gain of BSR cavity provide a new approach of reducing the shot noise, complementary to squeezing and increasing the power. A balance between the laser power and the signal recycling gain can provide an easier access to cryogenic techniques for reducing classical noises, *e.g.* cryogenic temperature which are proposed for LIGO Voyager [18], the Einstein Telescope low-frequency detector [19, 20], and Cosmic Explorer phase II [21].

ACKNOWLEDGEMENTS

T. Z., J.B. and H. M. acknowledge the support of the Institute for Gravitational Wave Astronomy at University of Birmingham. H. M. is supported by UK STFC Ernest Rutherford Fellowship (Grant No. ST/M005844/11).

[1] H. Miao, N. D. Smith, and M. Evans, Quantum limit for laser interferometric gravitational-wave detectors from optical dissipation, *Phys. Rev. X* **9**, 011053 (2019).

[2] J. Aasi, B. P. Abbott, R. Abbott, T. Abbott, et al., Advanced LIGO, *Classical and Quantum Gravity* **32**, 074001 (2015).

[3] H. Miao, H. Yang, and D. Martynov, Towards the design of gravitational-wave detectors for probing neutron-star physics, *Phys. Rev. D* **98**, 044044 (2018).

[4] D. Martynov, H. Miao, H. Yang, F. H. Vivanco, E. Thrane, R. Smith, P. Lasky, W. E. East, R. Adhikari, A. Bauswein, A. Brooks, Y. Chen, T. Corbitt, A. Freise, H. Grote, Y. Levin, C. Zhao, and A. Vecchio, Exploring the sensitivity of gravitational wave detectors to neutron star physics, *Phys. Rev. D* **99**, 102004 (2019).

[5] V. B. Braginsky, Y. I. Vorontsov, and K. S. Thorne, Quantum nondemolition measurements, *Science* **209**, 547 (1980).

[6] Y. Chen, S. L. Danilishin, F. Y. Khalili, and H. Müller-Ebhardt, QND measurements for future gravitational-wave detectors, *General Relativity and Gravitation* **43**, 671 (2011).

[7] H. J. Kimble, Y. Levin, A. B. Matsko, K. S. Thorne, and S. P. Vyatchanin, Conversion of conventional gravitational-wave interferometers into quantum nondemolition interferometers by modifying their input and/or output optics, *Phys. Rev. D* **65**, 022002 (2001).

[8] V. B. Adya, M. J. Yap, D. Töyrä, T. G. McRae, P. A. Altin, L. K. Sarre, M. Meijerink, N. Kijbunchoo, B. J. J. Slagmolen, R. L. Ward, and D. E. McClelland, Quantum enhanced kHz gravitational wave detector with internal squeezing, *Classical and Quantum Gravity* **37**, 07LT02 (2020).

[9] M. Korobko, L. Kleybolte, S. Ast, H. Miao, Y. Chen, and R. Schnabel, Beating the standard sensitivity-bandwidth limit of cavity-enhanced interferometers with internal squeezed-light generation, *Phys. Rev. Lett.* **118**, 143601 (2017).

[10] Y. Zhao, N. Aritomi, E. Capocasa, M. Leonardi, M. Eisenmann, Y. Guo, E. Polini, A. Tomura, K. Arai, Y. Aso, Y.-C. Huang, R.-K. Lee, H. Lück, O. Miyakawa, P. Prat, A. Shoda, M. Tacca, R. Takahashi, H. Vahlbruch, M. Vardaro, C.-M. Wu, M. Barsuglia, and R. Flaminio, Frequency-dependent squeezed vacuum source for broadband quantum noise reduction in advanced gravitational-wave detectors, *Phys. Rev. Lett.* **124**, 171101 (2020).

[11] L. McCuller, C. Whittle, D. Ganapathy, K. Komori, M. Tse, A. Fernandez-Galiana, L. Barsotti, P. Fritschel, M. MacInnis, F. Maticichard, K. Mason, N. Mavalvala, R. Mittleman, H. Yu, M. E. Zucker, and M. Evans, Frequency-dependent squeezing for advanced ligo, *Phys. Rev. Lett.* **124**, 171102 (2020).

[12] K. Ackley, V. B. Adya, P. Agrawal, P. Altin, G. Ashton, M. Bailes, E. Baltinas, A. Barbui, D. Beniwal, C. Blair, D. Blair, G. N. Bolingbroke, V. Bossilkov, S. S. Boublil, D. D. Brown, B. J. Burridge, J. C. Bustillo, J. Cameron, H. T. Cao, J. B. Carlin, A. Casey, S. Chang, P. Charlton, C. Chatterjee, D. Chattopadhyay, X. Chen, J. Chi, J. Chow, Q. Chu, A. Ciobanu, T. Clarke, P. Clearwater, J. Cooke, D. Coward, H. Crisp, R. J. Dattatri, A. T. Deller, D. A. Dobie, L. Dunn, P. J. Easter, J. Eichholz, R. Evans, C. Flynn, G. Foran, P. Forsyth, Y. Gai, S. Galaudage, D. K. Galloway, B. Gendre, B. Gonorcharov, S. Goode, D. Gozzard, B. Grace, A. W. Graham, A. Heger, F. H. Vivanco, R. Hirai, N. A. Holland, Z. J. Holmes, E. Howard, E. Howell, G. Howitt, M. T. Hübner, J. Hurley, C. Ingram, V. J. Hamedan, K. Jenner, L. Ju, D. P. Kapasi, T. Kaur, N. Kijbunchoo, M. Kovalam, R. K. Choudhary, P. D. Lasky, M. Y. M. Lau, J. Leung, J. Liu, K. Loh, A. Mailvagan, I. Mandel, J. J. McCann, D. E. McClelland, K. McKenzie, D. McManus, T. McRae, A. Melatos, P. Meyers, H. Middleton, M. T. Miles, M. Millhouse, Y. L. Mong, B. Mueller, J. Munch, J. Musiov, S. Muusse, R. S. Nathan, Y. Naveh, C. Neijssel, B. Neil, S. W. S. Ng, V. Oloworaran, D. J. Ottaway, M. Page, J. Pan, M. Pathak, E. Payne, J. Pow-

ell, J. Pritchard, E. Puckridge, A. Raidani, V. Rallabhandi, D. Reardon, J. A. Riley, L. Roberts, I. M. Romero-Shaw, T. J. Roocke, G. Rowell, N. Sahu, N. Sarin, L. Sarre, H. Sattari, M. Schiworski, S. M. Scott, R. Sengar, D. Shaddock, R. Shannon, J. SHI, P. Sibley, B. J. J. Slagmolen, T. Slaven-Blair, R. J. E. Smith, J. Spollard, L. Steed, L. Strang, H. Sun, A. Sunderland, S. Suvorova, C. Talbot, E. Thrane, D. Töyrä, P. Trahanas, A. Vajpeyi, J. V. van Heijningen, A. F. Vargas, P. J. Veitch, A. Vigna-Gomez, A. Wade, K. Walker, Z. Wang, R. L. Ward, K. Ward, S. Webb, L. Wen, K. Wette, R. Willcox, J. Winterflood, C. Wolf, B. Wu, M. J. Yap, Z. You, H. Yu, J. Zhang, J. Zhang, C. Zhao, and X. Zhu, Neutron star extreme matter observatory: A kilohertz-band gravitational-wave detector in the global network (2020), [arXiv:2007.03128 \[astro-ph.HE\]](https://arxiv.org/abs/2007.03128).

[13] R.-H. Rinkleff and A. Wicht, The concept of white light cavities using atomic phase coherence, *Physica Scripta* , **85** (2005).

[14] H. Miao, Y. Ma, C. Zhao, and Y. Chen, Enhancing the bandwidth of gravitational-wave detectors with unstable optomechanical filters, *Phys. Rev. Lett.* **115**, 211104 (2015).

[15] M. A. Page, M. Goryachev, H. Miao, Y. Chen, Y. Ma, D. Mason, M. Rossi, C. D. Blair, L. Ju, D. G. Blair, A. Schliesser, M. E. Tobar, and C. Zhao, Gravitational wave detectors with broadband high frequency sensitivity (2020), [arXiv:2007.08766 \[physics.optics\]](https://arxiv.org/abs/2007.08766).

[16] D. Mason, J. Chen, M. Rossi, Y. Tsaturyan, and A. Schliesser, Continuous force and displacement measurement below the standard quantum limit, *Nature Physics* **15**, 745 (2019).

[17] S. L. Danilishin, F. Y. Khalili, and H. Miao, Advanced quantum techniques for future gravitational-wave detectors, *Living Reviews in Relativity* **22**, 2 (2019).

[18] R. X. Adhikari, K. Arai, A. F. Brooks, C. Wipf, O. Aguiar, P. Altin, B. Barr, L. Barsotti, R. Bassiri, A. Bell, G. Billingsley, R. Birney, D. Blair, E. Bonilla, J. Briggs, D. D. Brown, R. Byer, H. Cao, M. Constance, S. Cooper, T. Corbitt, D. Coyne, A. Cumming, E. Daw, R. deRosa, G. Eddolls, J. Eichholz, M. Evans, M. Fejer, E. C. Ferreira, A. Freise, V. V. Frolov, S. Gras, A. Green, H. Grote, E. Gustafson, E. D. Hall, G. Hammond, J. Harms, G. Harry, K. Haughian, D. Heinert, M. Heintze, F. Hellman, J. Hennig, M. Hennig, S. Hild, J. Hough, W. Johnson, B. Kamai, D. Kapsi, K. Komori, D. Koptsov, M. Korobko, W. Z. Korth, K. Kuns, B. Lantz, S. Leavay, F. Magana-Sandoval, G. Mansell, A. Markosyan, A. Markowitz, I. Martin, R. Martin, D. Martynov, D. E. McClelland, G. McGhee, T. McRae, J. Mills, V. Mitrofanov, M. Molina-Ruiz, C. Mow-Lowry, J. Munch, P. Murray, S. Ng, M. A. Okada, D. J. Ottaway, L. Prokhorov, V. Quetschke, S. Reid, D. Reitze, J. Richardson, R. Robie, I. Romero-Shaw, R. Route, S. Rowan, R. Schnabel, M. Schneewind, F. Seifert, D. Shaddock, B. Shapiro, D. Shoemaker, A. S. Silva, B. Slagmolen, J. Smith, N. Smith, J. Steinlechner, K. Strain, D. Taira, S. Tait, D. Tanner, Z. Tornasi, C. Torrie, M. V. Veggel, J. Vanheijningen, P. Veitch, A. Wade, G. Wallace, R. Ward, R. Weiss, P. Wessels, B. Willke, H. Yamamoto, M. J. Yap, and C. Zhao, A cryogenic silicon interferometer for gravitational-wave detection, *Classical and Quantum Gravity* **37**, 165003 (2020).

[19] The ET Science Team, [Einstein gravitational wave Telescope conceptual design](https://cds.cern.ch/record/2200000) (European Commission, 2011).

[20] ET Steering Committee Editorial Team, [Einstein Telescope design report update 2020](https://cds.cern.ch/record/2200000) (Einstein Telescope Collaboration, 2020).

[21] B. P. Abbott, R. Abbott, T. D. Abbott, M. R. Abernathy, K. Ackley, C. Adams, P. Addesso, R. X. Adhikari, et al., Exploring the sensitivity of next generation gravitational wave detectors, *Classical and Quantum Gravity* **34**, 044001 (2017).